10th International Conference on Composite Science and Technology
ICCST/10
A.L. Araújo, J.R. Correia, C.M. Mota Soares, et al. (Editors)

EFFECT OF SILICON CARBIDE NANOPARTICLES ON CRYSTALLINITY OF WATERBORNE POLYURETHANE

Renata Patrícia dos Santos[*], Silvana Navarro Cassu[*†], Cristina Moniz Araujo Lopes [*†]

[*]Instituto Tecnológico de Aeronáutica (ITA)
Pça Marechal Eduardo Gomes, 50, São José dos Campos - 12228-900 - Brasil
renata_patricia2003@yahoo.com.br

[†] Instituto de Aeronáutica e Espaço (IAE)
Pça. Marechal Eduardo Gomes, 50-S. José dos Campos - 12228-904- Brasil
silvanasnc@iae.cta.br, cristinacmal@iae.cta.br

Key words: Nanocomposite, Ceramic nanoparticles, Impact energy absorption

Summary:

Inter-yarns and inter-layers friction influences the capacity of high velocity impact energy absorption of multilayered fabrics composites. One of the alternatives to tune levels of friction and, consequently, levels of filament mobility in such composites is by modifying matrix by hard nanofillers addition. In this study we focused in investigating the effect of silicon carbide (SiC) nanoparticles (10 nm) on the crystallinity of aliphatic polyester polyurethane (PU) used as matrix for Kevlar laminated fabrics. The addition of the particles to semi-crystalline polymers may interfere in the degree of crystallinity, phase morphology, size and size distribution of crystalline phase depending on the polymer-particle interaction. The effect of the addition of ceramic nanoparticles on the crystalline phase of aliphatic polyester polyurethane (PU) was evaluated by differential scanning calorimetry (DSC) and x-ray diffraction (XRD). Aqueous and acetone β-SiC slurry were introduced to a waterborne anionic dispersion of high molar weight PU, stirred and homogenized with ultrasonic power. Thin films with up to 0.5 wt% of SiC were prepared by casting method. Microscopy analysis suggested improvement in dispersion of organosilane surface modified nanoparticles compared to nanoparticles without treatment. Evaluation of both surfaces of casted nanocomposites film by UATR/FT-IR evidenced more homogeneous films from acetone β-SiC slurry, what might be a consequence of the smaller particles size distribution found in acetone detected by DLS and higher stability of nanoparticles suspension. Results shown that the addition of acetone to the neat waterborne PU ($PU_{(acetone)}$) causes a delay in crystals formation and β-SiC nanoparticles act as nucleating agent favoring crystallization. A shift of crystallization temperature towards the crystalline phase melting temperature was observed for the nanoparticles filled polymer.

INTRODUCTION

Polymeric fibers with high modulus as ultra-high molecular weight polyethylene (UHMWPE) and *p*-aramid are capable of absorbing high impact energy [1, 2]. The main mechanism to absorb impact energy wave propagation in fabric laminates is fiber deformation and/or breakage. Another import factor that will influence the energy dissipation mechanism is the friction forces. Studies have shown that increasing friction between filaments of the fabrics might lead to increase energy dissipation efficiency [3-5]. Bazhenov and Goncharuk [4] studied the dissipation forces in p-aramid fabric and concluded that waving patterns that resulted in higher interyarn friction were more effective. Karthikeyan et al. [5] noticed that different matrices result in different interlayer friction changing the dynamic shear of Ultra High Molecular Weight Polyethylene (UHMWPE) laminates.

Another way to improve the impact resistance is adding reinforcement on the matrix by incorporating nanoparticles [6-9]. Obradovic et al. achieved better impact properties by impregnating p-aramid fabric/polyurethane with carbon nanotube covered with silane [7] and aramid fabrics impregnated with 30% silane modified nanosilica [9] compared to the same systems without nanoparticles.

Incorporating nanoparticles in a polymeric system has been extensively studied in the last years. The microfillers are been replaced by nanofillers because particles in nano scale have higher interfacial polymer/filler area were interaction are established, therefore the contribution to improve the mechanical properties is more significant [10]. Since in semicrystalline polymers the crystalline phase plays an important role in mechanical properties, it is also import to evaluate how modification with fillers affects crystallinity. Blagojević et al. [10] investigated the mechanical properties of polyurethane rubber (PUR)/nanosilica without and with two types of silanes (methacrylsilane and octylsilane) by isothermal crystallization kinetic using DSC and they shown that the content of nanosilica affected the crystallization behavior of PUR. Das et al [11] observed more intense PU peaks in XRD analysis of PU/MWCNT nanocomposite due to the nucleation effect regarding to MWCNT presence.

For this study we selected beta silicon carbide (β-SiC) nanoparticles because of their excellent properties as high elastic modulus and hardness, good thermal and chemical stability making them an attractive alternative[12]. Hard particles may enable to modify the friction force in a fabric to improve impact absorption. Polyurethane (PU) matrix has resiliency and flexibility to encapsulate fibrous components what is an important requirement to prepare multilayered fabrics composites capable of absorbing high impact energy [13]. The aim of this work is testing different systems to effectively incorporate β-SiC nanoparticles to aliphatic polyester PU and investigating the effect of nanofillers on the crystallinity of the nanocomposite, used as matrix for Kevlar laminated fabrics.

MATERIALS AND METHODS

Thermoplastic aliphatic polyurethane (PU) in water dispersion, Dispercoll U-54® produced by Bayer Germany, was used as matrix for preparation of the neat PU and $\text{PU}_{(\text{acetone})}$ films and for preparation of polyurethane/β-silicon carbide (PU/β-SiC) nanocomposites. Dispercoll U-54® has solid material content between 49 and 51%, viscosity ranging from 40 to 600 mPa.s, and pH between 6.0 and 9.0.

Beta silicon carbide nanoparticles, β-SiC (cubic crystal structure [14]) manufactured by

Nanostructured & Amorphous Materials Inc., was used as filler. According to manufacturer specifications, the particles size is 10 nm (APS) and purity 97%.

The surface of silicon carbide nanoparticles was modified with the 3-aminopropyltrimethoxysilane (*APTS*) organossilane coupling agent supplied by Aldrich. The reaction (1:2 APTS/SiC molar ration), was carried out in ethanol medium under reflux at 82 °C for 5 hours.

Dispersion preparation

PU/β-SiC nanocomposites were prepared from two different methods. In the first (process 1) β-SiC nanoparticles were dispersed in water under stirring and ultrasound bath simultaneously by 30 minutes. Dispercoll U-54® was added to the dispersion and the same previous homogenization procedure was repeated, followed by extra 30 minutes of stirring, without ultrasound.

In the second process (process 2) used to prepare PU/β-SiC nanocomposites, β-SiC was dispersed in acetone; this suspension was stirred by 30 minutes, and after it was stirred and ultrasound bath simultaneously by 1 hour. The ceramic suspension was added to Dispercoll and the mixture was kept under stirring and ultrasonication simultaneously by 15 minutes, followed by extra 15 minutes of stirring. All formulations prepared are shown in **Table 1**.

Table 1: Dispersion formulations used to prepare neat PU, PU $_{(acetone)}$ and PU/β-SiC nanocomposites. [a]The same amount of acetone used to prepare $D_{AcSiC\ 0.1\%}$ was also added the $_{PU(acetone)}$.

Nanocomposite	Medium	β-SiC (wt%)	β-SiC silanized (wt%)	Process
Neat PU	---	---	---	---
PU $_{(acetone)}$[a]	Acetone	---	---	---
$D_{WSiC\ 0.1\%}$	Water	0.1	---	1
$D_{WSiC\ 0.5\%}$	Water	0.5	---	1
$D_{WSiC\ Mod\ 0.5\%}$	Water	---	0.5	1
$D_{Ac\ SiC\ 0.1\%}$	Acetone	0.1	---	2

Film preparation

Neat PU, $PU_{(acetone)}$ and PU/ β-SiC nanocomposites films were prepared by solvent casting. The dispersion was poured in silicone plates and after 3 hours the plates were placed under vacuum in desiccators, remaining for 24 hours. The resultant films were heated for 1 hour at 100 °C to ensure solvents were removed.

Characterization

PU/β-SiC nanocomposite films surfaces were characterized by Fourier transform infrared spectroscopy (FT-IR) using spectrometer Perkin Elmer Spectrum One, resolution 4 cm $^{-1}$, gain 1, spectral range 4000-550 cm^{-1}, reflection techniques ATR with Ge crystal at 45° angle, universal accessory UATR containing ZnSe and diamond and force of 120 N.

Micrographs were obtained by scanning electron microscopy (SEM) from the secondary electrons (SEI) using LEO 435 VPI- SE with accelerating voltage of 20 kV.

Crystallinity of PU/β-SiC nanocomposite films were evaluated by X-ray diffraction (XRD) at room temperature (~25 ºC) with a Philips/PANalytical, model X'Pert PRO MPD 3060, with scan from 5º to 90º, power 40 kV and 45 mA, CuKα radiation, step size of 0.0167 Å, step time of 5 seconds. The graphics were generated using software High Score Plus (Philips) and JCPDS-ICDD standards.

PU/β-SiC nanocomposites films were evaluated by differential scanning calorimetry (DSC) in a DSC Q100 TA Instruments. These analysis were carried out from -90 °C to 200 °C (heating rate 10 °C.min^{-1}), under a nitrogen atmosphere (50 ml.min^{-1}), in an aluminum crucible. The cooling was conducted from 200 °C to -90 °C (cooling rate of 10 °C.min^{-1}) and the second heating was from -90 °C to 200 ° C (heating rate of 10 °C.min^{-1}).

Nanoparticles size distribution was evaluated using the dynamic light scattering (DLS) analysis. The particles were dispersed in water or acetone, to understand the solvent influence. These dispersions remained under magnetic stirring for 30 minutes and extra 30 minutes in an ultrasound bath to deagglomeration of the particles.

RESULTS AND DISCUSSION

Homogeneity evaluation of PU/β-SiC films from aqueous slurry -0.5 SiC %

Figure 1 shows a comparison of the micrographs of PU/β-SiC film prepared with β-SiC (**Figure 1-a**) and silane-modified β-SiC (**Figure 1-b**) water slurries. PU film obtained with β-SiC presented a large particle size distribution with agglomerates larger than 1μm, which indicates that water without dispersant was not efficient to promote the breakage of the β-SiC agglomerates. However, PU/β-SiC film containing silane-β-SiC, $D_{WSiCMod\ 0.5\%}$ (**Figure 1-b**) shows better β-SiC particles distribution in PU matrix when compare with $D_{WSiC\ 0.5\%}$. It can be attributed to the better interaction between polymer and filler due to the silanization of the surface of β-SiC particles.

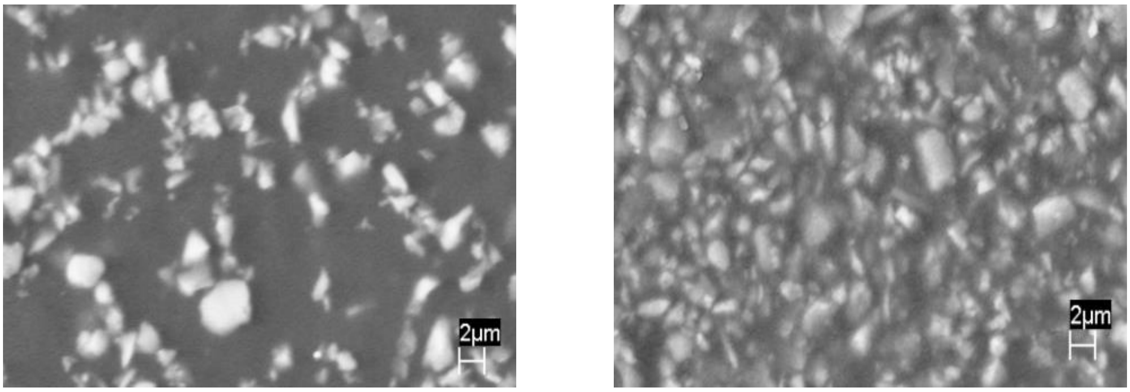

(a) **(b)**

Figure 1: SEM micrograph of PU/β-SiC nanocomposites films micrographs of dispersions (a) $D_{WSiC\ 0.5\%}$, (b) $D_{WSiCMod\ 0.5\%}$, both 3000 times magnification.

Due to the poor dispersion of β-SiC observed for the PU/β-SiC nanocomposites films by

SEM, their surfaces (front and back face) were also analyzed by UATR/ FT-IR to investigate sedimentation and homogeneity of the film nanocomposite film. **Figure 2** shows the FT-IR spectra of neat PU, β-SiC particles and PU/β-SiC nanocomposites films: $D_{WSiC\ 0.5\%}$ and $D_{WSiCMod\ 0.5\%}$. Absorptions related to PU are identified by NH bands between 3390-3330 cm^{-1}; CN and NH between 1530-1520 cm^{-1}; a carbonyl band (C=O) at 1726 – 1725 cm^{-1} attributed to free ester and/or urethane [15]; an absorption between 1260-1250 cm^{-1} assigned to ester; a band between 1120-1110 cm^{-1} attributed to (CO) from ether, indicating that PU may be a polyether or a mixture of both [16], although ether band intensity is higher than ester band. β-SiC spectrum presented bands in the region of 1052 cm^{-1} assigned to the Si-O-Si and at approximately 780 cm^{-1} attributed to Si-C [14]. SiC surface usually presents an oxygen-rich layer, chemically similar to the silica surface, which explain the presence of Si–O absorptions in β-SiC FT-IR spectrum [17].

Comparing PU/β-SiC nanocomposite films spectra of both sides, front and back face, a clear difference is observed. In the back face of nanocomposites, besides PU characteristic bands widening bands in the region of 770-900 cm^{-1} are also detected indicating the β-SiC presence. Another difference can be noticed at the 2330-1900 cm^{-1}region, which presents interference due to refractive index of the crystal and the β-SiC, hence this region should be not used to characterize the material.

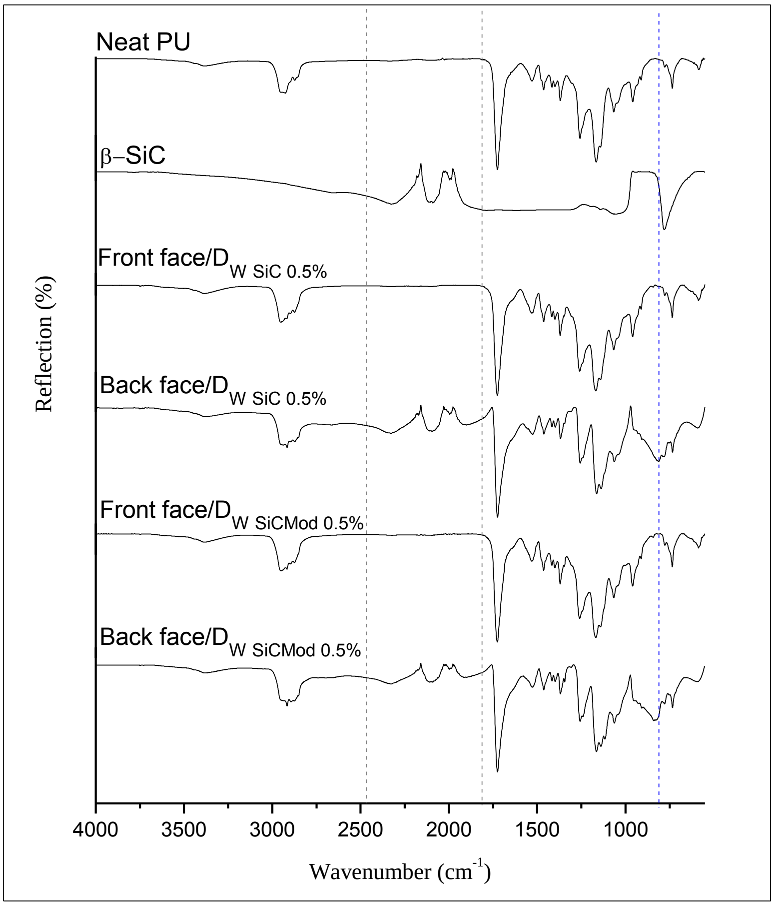

Figure 2: UATR/FT-IR spectra of film surface obtained from neat PU, β-SiC nanoparticles, back and front face of the PU/β-SiC nanocomposites $D_{WSiC\ 0.5\%}$ and $D_{WSiCMod\ 0.5\%}$.

SEM micrographs and UATR/FT-IR spectra performed for PU/β-SiC films shown that β-SiC agglomeration was not broken in water dispersion, which resulted in its poor dispersion in the PU films.

Influence of solvent on dispersion stability and particle size - 0.1 SiC %

Since the aqueous slurry process was not efficient to obtain homogeneous and stable nanocomposite films, dispersion another β-SiC slurry was prepared using acetone as an attempt to prevent the nanoparticles aggregation and sedimentation to promote better stability to the system.

Dispersion stability was evaluated by visually monitoring sedimentation through time. **Figure 3** compares pictures of dispersions, $D_{WSiC\ 0.1\%}$ and $D_{AcSiC\ 0.1\%}$, prepared with water and acetone, respectively. The images were registered immediately (**Figure 3-a**, **Figure 3-c**) and 24 hours after dispersion preparation (**Figure 3-b**, **Figure 3-d**). The visual aspect suggests that the process 2, using acetone to prepare the β-SiC slurry ($D_{AcSiC\ 0.1\%}$) does not present any β-SiC sedimentation, which can be attributed to the better β-SiC dispersion in acetone. The opposite behavior was observed for $D_{WSiC\ 0.1\%}$, that the sedimentation is pronounced, as shown in the **Figure 3-b,** which can be attributed to the larger β-SiC agglomerate in water dispersion.

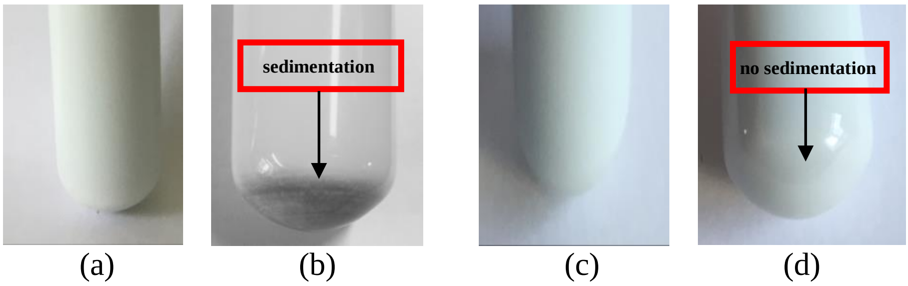

Figure 3: Visual aspect of dispersions focusing on sedimentation. $D_{WSiC\ 0.1\%}$:(a) immediately and (b) after 24 hours of preparation; $D_{Ac\ SiC\ 0.1\%}$:(c) immediately and (d) after 24 hours of preparation.

Particle size distribution analysis confirmed that β-SiC size was smaller in acetone than in water dispersion, which was observed in D50, D10 and D90 indicating that 10%, 50%, 90%, respectively, of particle sizes will be found below the value described in the **Table 2**.

Table 2: Particle size distributions of β-SiC in water and acetone

Suspension medium	D50 (nm)	D10 - D90 (nm)
Water	1114.4	359.5 - 3729.0
Acetone	179.5	67.3 - 545.7

Homogeneity evaluation of PU/β-SiC films from acetone slurry - 0.1 SiC %

From the previous results it was expected that acetone slurry with 0.1% of SiC would result in homogeneous nanocomposite films. For confirm that PU/β-SiC nanocomposites, $D_{AcSiC\ 0.1\%}$, were analyzed by UATR/FT-IR (**Figure 4**). To compare PU film to PU/β-SiC nanocomposites, the same amount of acetone that was used to prepare $D_{AcSiC\ 0.1\%}$ was also added to neat PU ($PU_{acetone}$). $D_{AcSiC\ 0.1\%}$ film presented similar absorptions observed for PU film prepared only by the solvent casting. It was not possible to detect spectrometric alterations influenced by the β-SiC presence. However, the FT-IR spectra of front and back face were similar and β-SiC characteristic absorptions were not observed. This result indicates better incorporation of filler into PU dispersion, due to the initial more efficient β-SiC particles dispersion in acetone preventing particles sedimentation, in accordance with DLS measurements and the stability evaluation.

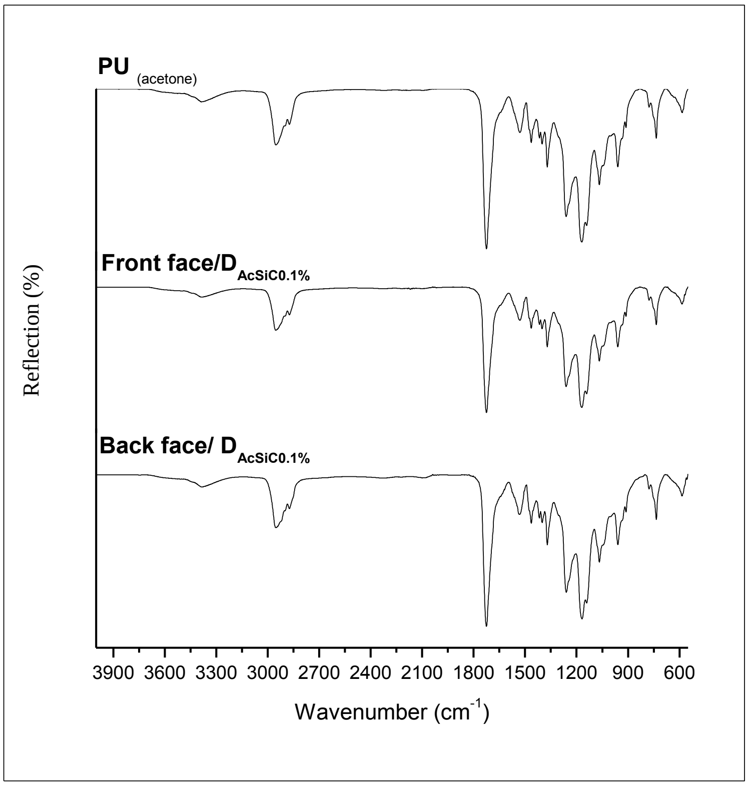

Figure 4: UATR/FT-IR spectra of front and back face of film obtained from dispersion of PU $_{(acetone)}$ and $D_{AcSiC\ 0.1\%}$.

Crystallinity study of neat PU, $PU_{(acetone)}$, PU/β-SiC nanocomposite ($D_{AcSiC\ 0.1\%}$) films

Polyurethane is a semi crystalline polymer with hard segment that provide strengthens to material and soft segment imparting elastomeric characteristics to these polymers. Generally in PU, organized microdomains are formed due to the chemical incompatibility between these segments [18]. These regions might be crystalline exhibiting spherulites in varied sizes according as found by Xu et al. [19]. The effect of acetone and β-SiC particles in PU crystallinity was evaluated by DSC and XRD, however, only the nanocomposite $D_{AcSiC\ 0.1\%}$ was studied due to its more homogeneous dispersion and because this nanocomposite does not presented β-SiC sedimentation.

DSC results are presented in **Figure 5** and **Table 3**. Comparing neat PU and $PU_{(acetone)}$ films, the addition of acetone causes a delay in crystals formation, resulting in a partial crystallization during the cooling. The crystallization is completed during the second heating (**Figure 5-a** and **5-b)**, however, the enthalpy values of melting and crystallization were similar to the neat PU and the PU$_{(acetone)}$ films, showing that the degree of crystallinity was not affected by addition of acetone (**Table 3**). When comparing the neat PU and PU$_{(acetone)}$ films with D$_{AcSiC\ 0.1\%}$, it was observed that crystallization occurs during cooling as observed for neat PU film, which suggests that the presence of the β-SiC nanoparticles acts as a nucleating agent favoring the PU crystallization even in presence of acetone. Blagojević et al. [10] investigated the influence of silica nanofiller added to linear hydroxyl polyester urethane (PUR) by isothermal crystallization kinetic (DSC) and noticed that the particles in content up to 1% vol. acted as nuclei and accelerated PUR crystallization.

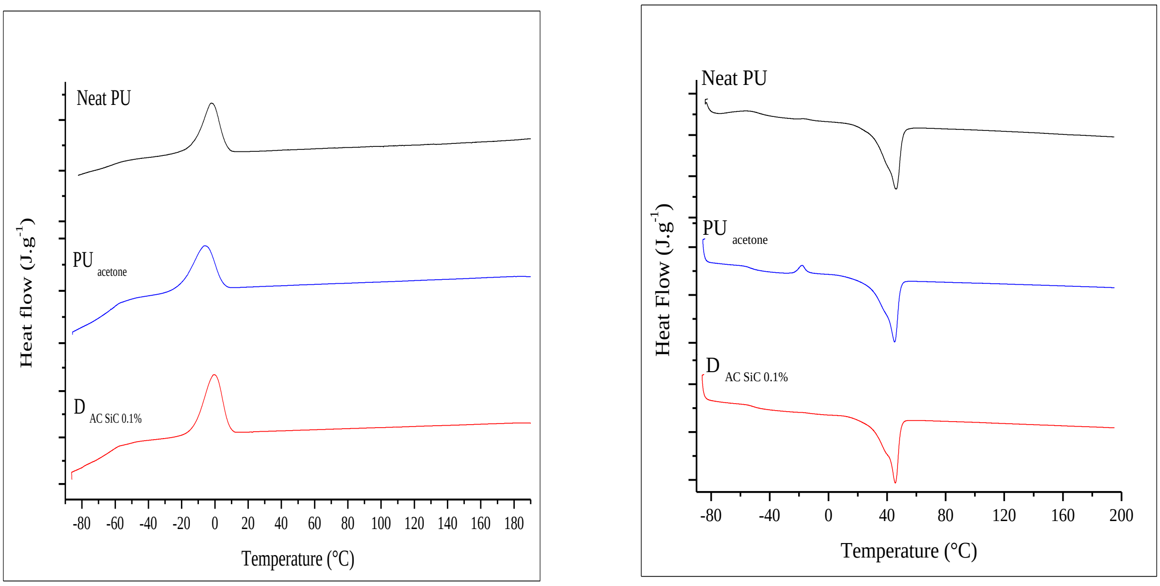

(a) **(b)**

Figure 5: DSC curves of (a) cooling and (b) second heating of neat PU, PU $_{(acetone)}$ and D$_{AcSiC0.1\%}$ films.

Table 3: DSC results for Neat PU, PU$_{(acetone)}$ and D$_{AcSiC\ 0.1\%}$ films.
^{a}The enthalpy of crystallization and melting were corrected in relation to PU content.

	COOLING			**HEATING**		
	Neat PU	PU $_{(acetone)}$	D$_{AcSiC\ 0.1\%}$	Neat PU	PU $_{(acetone)}$	D$_{AcSiC\ 0.1\%}$
ΔH$_c$ (J/g)^a	34.1 ± 1	27 ± 3	33 ± 1	---	2.6 ± 2.4	---
T$_c$ (°C)	-2.3 ± 0.5	-6.4 ± 0.8	-1 ± 3	---	-17.9 ± 0.3	---
ΔH$_m$ (J/g)^a	---	---	---	36 ± 1	38 ± 1	38 ± 1

Figure 6 shows the X-ray diffraction curves of β-SiC, neat PU, PU$_{(acetone)}$ and D$_{AcSiC\ 0.1\%}$ films. The XDR of β-SiC shown a characteristic pattern peaks at 2θ = 35.7 °, 2θ = 41.5 °, 2θ = 60.0 °, 2θ = 71.8 °and 2θ = 75.5 °. The neat PU film presented peaks at 2θ = 21.3° and 2θ

= 24.3°. The addition of acetone to neat PU, $PU_{(acetone)}$, caused a shift in peaks in relation to that observed for neat PU, which were observed at 2θ = 21.8° and 24.1°. Moreover, the relative peaks intensity was changed as can be observed in **Figure 6**. Another difference observed in X-ray diffraction curve of $PU_{(acetone)}$ film was the presence of a peak at 2θ = 22.4°, which was not observed in the neat PU film. This modification in $PU_{(acetone)}$ XRD difratogram shows the interference caused by the acetone addition in neat PU crystallinity, in accordance with it was observed by DSC results. The $D_{AcSiC\ 0.1\%}$ XRD presented characteristic peaks at the same 2θ observed for $PU_{(acetone)}$, however, the intensity of the peak at 2θ = 21.8° was remarkable increased, indicating that the β-SiC particles acted as a nucleating agent for PU chains. A similar behavior was observed by Das et al. [11]. These authors incorporated multi-walled carbon nanotube (MWCNT) in PU matrix, and the nanocomposite did not present MWCNT peaks in XRD, but a higher intensity PU peaks was found by nucleating effect.

Comparing the XRD of $D_{AcSiC\ 0.1\%}$ and $PU_{(acetone)}$ is not possible to find β-SiC peaks, confirming the homogeneity of β-SiC particles dispersion in PU matrix.

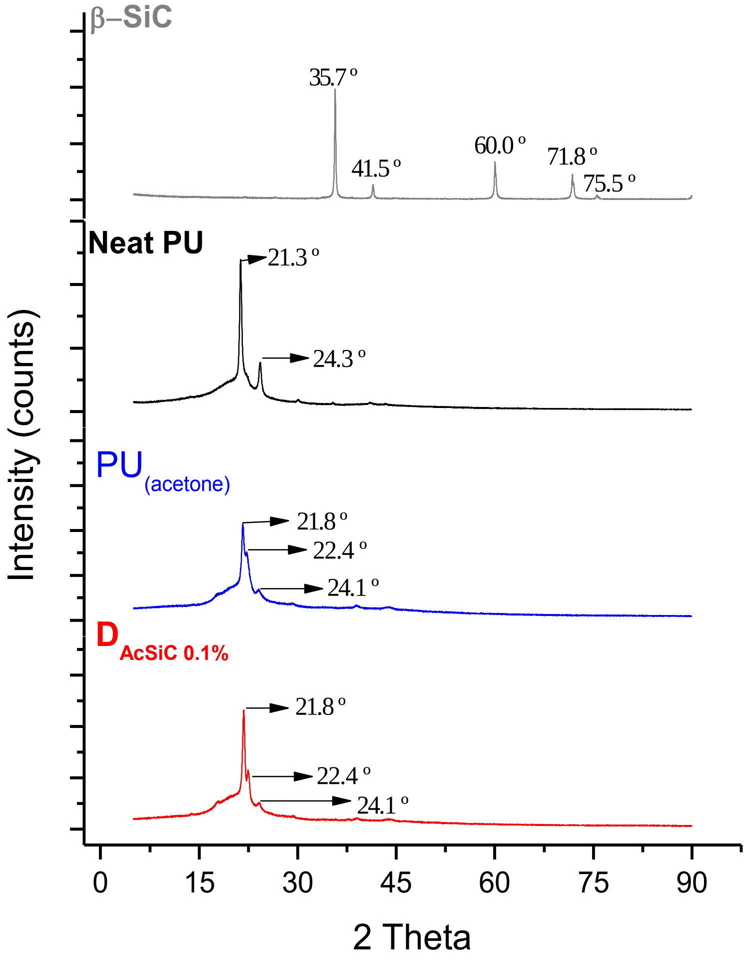

FIGURE 6: XRD curves of β-SiC, $PU_{(acetone)}$, $D_{AcSiC\ 0.1\%}$ and neat PU films.

CONCLUSIONS

PU/β-SiC nanocomposites were prepared using β-SiC particles dispersed in water or in acetone. SEM micrographs and UATR/FT-IR spectra shown agglomeration and sedimentation of β-SiC particles in PU/β-SiC nanocomposites obtained with β-SiC water suspension. The addition of acetone to neat PU, $PU_{(acetone)}$, changed the behavior of PU crystallization, however, the crystallization and melting enthalpy were similar to that observed for neat PU. Homogeneous and more stable dispersion of β-SiC were reached with acetone as dispersant, which results in homogenous PU/β-SiC nanocomposite film. The influence of β-SiC particles in this nanocomposite was monitored by DSC and XRD, which shown that crystallization was changed in presence of β-SiC particles, which acted as a nucleating agent.

ACKNOWLEDGMENTS

The authors acknowledge to FINEP (01.12.0211.00) and CNPq (382575 / 2014-8).

REFERENCES

[1] M.J.N. Jacobs, J.L.J. Van Domgemem, Ballistic protection mechanisms in personal armour. *Journal of Materials Science*, **36**, p. 3137 – 3142, 2001.

[2] M. Grujicic, G. Arakere, T. He, W.C. Bell, B.A. Cheeseman, C. F. Yen, B. Scott, A ballistic material model for cross-pied unidirectional ultra-high molecular-weight polyethylene fiber-reinforced armor-grade composites. *Material Science and Engineering A*, **498**, p. 231-341, 2008.

[3] J. Li, F. B.Ye, Effect of surface modification of Kevlar fibre on friction and wear properties of UHMWPE composites. *Plastics, Rubber and Composites*, **39**, n. 6, p. 264-267, 2010.

[4] S.L. Bazhenov, G.P. Goncharuk, A study of yarn friction in Aramid fabrics. *Polymer Science*, **54**, p. 1532 – 1538, 2012.

[5] K. Karthikeyan, B.P. Russel,; N.A. Fleck, H.N.G Wadley, V.S. Deshpande, The effect of shear strength on the ballistic response of laminated composite plates. *European Journal of Mechanics- A/Solids*, **42**, p. 35-53, 2013.

[6] H. Mahfuz, F. Clements, V. Rangari, V. Dhanak, G. Beamson, Enhanced stab resistance of armor composites with functionalized silica nanoparticles. *Journal of Applied Physics***,** **105**, p.064307-1 – 064307-7, 2009.

[7] V. Obradović, D. Stojanović,; M. Grković, I. Živković, V. Radojević, P. Uskoković, R. Alksic, Dynamic mechanical properties of aramid fabrics impregnated with carbon nanotube/ poly (vinyl butyral)/ethanol solution. *Metall. Metar. Eng.*, **19**(3), p. 259 – 266, 2013.

[8] P.N.B. Reis, J.A.M. Ferreira, Z. Y. Zhang, T. Benameur, M.O.W. Richardson, Impact response of kevlar composites with nanoclay enhanced epoxy matrix, **46**, *Composites: Part B*, p. 7-14, 2013.

[9] V. Obradović, D.B. Stojanović, R. Janeié-Heinemann, I. Živković, V. Radojević, P.S. Uskoković, R. Aleksié, Ballistic Properties of Hybrid Thermoplastic Composites with Silica Nanoparticles. *Journal of Engineered Fibers and Fabrics*, **9**, p. 97-107, 2014.

[10] S.L. Blagojević, Z. Buhin, I. Igrec, Influence of Silica Nanofiller on the Isothermal

Crystallization and Melting of Polyurethane Elastomer. *Journal of Applied Polymer Science*, **129**, p. 1466-1475, 2012.

[11] B. Das, P. Chattopadhyay, D. Misha, T.K. Maiti, S. Maji, R. Narayan, N. Karak. K., Nanocomposites of bio-based hyperbranched polyurethane/funtionalized MWCT as non-immunogenic, osteoconductive, biodegradable and biocompatible scaffolds in bone tissue engineering. *Journal of Materials Chemistry B*, **1**, p. 4115-4126, 2013.

[12] H.N. Yoshimura, A.C. da Cruz, Sintering of 6H(α) and 3C(β)-SiC powders with B_4C and C additives. *Journal of Materials Science*, **37**, p. 1541-1546, 2002.

[13] B.P. Russell, K. Karthikeyan, V.S. Deshpande, N.A. Fleck, The high strain rate response of Ultra High Molecular-weight Polyethylene: From fibre to laminate. *International Journal of Impact Engineering*, **20**, p. 1-9, 2013.

[14] N. Nikkam, M. Saleemi, E.B. Haghighi, M. Ghanbarpour, R. Khodabandeh, M. Muhammed, B. Palm, M.S. Toprak, Fabrication, characterization and thermophysical property evaluation of SiC nanofluids for heat transfer applications. *Nano-Micro Lett*, **6**, p. 178-189, 2014.

[15] A.L. Smith, *Applied infrared spectroscopy*. New York: John Wiley & Sons, 1979. 286p.

[16] J. Urbanski, et al. (Ed.), *Handbook of analysis of synthetic polymers and plastics*. New York: John Wiley & Sons, 1977.

[17] B.P. Singh, J. Jena, B. Bhattacharjee, S. Bhattacharjee, Dispersion of nano-silicon carbide (SiC) powder in aqueous suspension. *Journal of Nanoparticle Research*, n. 9, p. 797-806, 2007.

[18] E. Princi, S. Vicini, P. Stagnaro, L. Conzatti. The nanostructured morphology of linear polyurethanes observed by transmission electron microscopy. *Micron*, **42**, p. 3-7, 2011.

[19] M.X. Xu, W.G. Liu, C.L. Wang, Z.X. Gao, K. Yao, Surface Crystalline Characteristics of Polyurethane Investigated by Atomic Force Microscopy. *Journal of Applied Polymer Science*, **61**, p. 2225-2228, 1996.